

Diameter-Controlled Vapor–Solid Epitaxial Growth and Properties of Aligned ZnO Nanowire Arrays

Jianye Li,^{*,†} Qi Zhang,[‡] Hongying Peng,^{§,||} Henry O. Everitt,^{§,⊥,*} Luchang Qin,[‡] and Jie Liu^{†,*}

Department of Chemistry and Department of Physics, Duke University, Durham, North Carolina 27708, and Department of Physics and Astronomy, University of North Carolina at Chapel Hill, Chapel Hill, North Carolina 27599

Received: September 20, 2008; Revised Manuscript Received: January 23, 2009

A facile, template-free method was used to grow large areas of well-aligned ZnO nanowire arrays on amorphous SiO₂ substrates. The arrays are composed of vertically aligned, single-crystalline, wurtzitic [001] ZnO nanowires whose diameters were easily controlled by growth temperature, adjusted by changing the distance between the substrate and the precursor material in the growth chamber. A vapor–solid epitaxial growth mechanism is proposed by which ZnO nanocrystals, nucleated on a NiO catalytic film, seed the growth of the ZnO nanowires. Photoluminescence spectra indicate broad visible wavelength emission, likely caused by near surface traps, whose intensity relative to band edge ultraviolet emission grows as nanowire radii decrease. UV photoconductivity measured for individual ZnO nanowire devices demonstrates their potential as a UV light nanosensor.

Introduction

Wurtzitic zinc oxide is a direct, wide band gap semiconductor that has attracted tremendous research interest for its unique properties and potential application in low-voltage, short wavelength (ultraviolet or green/blue) electro-optical devices, chemical sensors, and varistors.^{1–5} In recent years, increasing attention has been focused on the study of ZnO nanowires/nanorods^{6–9} and other nanostructures^{10–13} for their great prospects in fundamental physical science, novel nanotechnological applications, and significant potential for nano-optoelectronics. For example, nano-ZnO was suggested to be the next most important nanomaterial after carbon nanotubes.¹⁴

Aligned ZnO nanowire arrays have been proposed for optoelectronics, sensing, field emission,⁸ dye-sensitized solar cells,¹⁵ and piezoelectric nanogenerators.¹⁶ For the most part, these aligned ZnO nanowire arrays have been grown on single-crystalline substrates like sapphire,^{1,8,9,17–25} but these substrates are much more expensive than amorphous substrates like silicon oxide, so their commercial potential has been limited. Here we report a facile, template-free method for growing vertical, well-aligned, high-density ZnO single-crystalline nanowire arrays on wafer-scale amorphous SiO₂ substrates. We report, perhaps for the first time for the method used, that growth sites and diameters of the vertically aligned ZnO nanowires were easily controlled, providing a economical approach to facilitate the development of large-scale ZnO nanowire-based nanodevices. Toward that end, the structural, optical, and electrical properties, as well as the growth mechanism, of the aligned ZnO nanowire arrays were investigated, and our results are reported here.

Experimental Section

The vertically aligned ZnO nanowire arrays were grown in a horizontal fused quartz tube inside a furnace originally designed to grow GaN nanowires.²⁶ The raw material was a mixture of ZnS (99.99%, Alfa Aesar) and graphite carbon powders (99.9995%, Alfa Aesar), used to lower the growth temperature, with a weight ratio of 2.6:1. A polished, 1.3 cm × 5 cm amorphous SiO₂ wafer (i.e., a silicon wafer with 1 μm thick amorphous thermal oxide) was cut into four ~1.5 cm² substrates. The substrates were catalyst-patterned by physically writing on them with an iron rod coated with a Ni(NO₃)₂ solution.²⁶ The precursor raw material and the catalyst-patterned substrates were loaded into a fused quartz boat in which the substrates were separated from the precursors by 5–10 cm. The boat was then placed into the horizontal fused quartz tube so that the raw material was located at the center where the temperature was highest. The tube was not sealed tightly so that air (oxygen) could enter the tube and completely oxidize ZnS to ZnO during the growth process. Then the furnace was heated under a steady flow of argon (99.99%, National Specialty Gases) with ~50–150 standard cubic centimeters per minute (sccm). When the center temperature reached 900 °C, the substrate temperatures were measured to decrease with distance from 889 °C at 5 cm to 833 °C at 10 cm. During growth these temperatures were held constant for 4–6 h, then the furnace was switched off and allowed to cool to room temperature quickly. The as-grown products were characterized by field emission scanning electron microscopy (FESEM, Philips FEI XL30SFEG), X-ray powder diffraction (XRD, Rigaku Multiflex X-ray diffractometer with Cu Kα radiation at room temperature), transmission electron microscopy (TEM, JEM 2010F), and photoluminescence (PL, excited by a He–Cd laser operating at 3.815 eV (325 nm) and measured by a grating spectrometer with a photomultiplier detector).

The individual ZnO nanowire devices were fabricated by an e-beam lithographic technique²⁷ as follows. First, n-type silicon wafers with 1 μm thick thermal oxide (Silicon Quest) were cleaned using a hot piranha solution (1 part concentrated H₂O₂

* Corresponding authors, jianyeli@hotmail.com, everitt@phy.duke.edu, and jliu@chem.duke.edu.

[†] Department of Chemistry, Duke University.

[‡] Department of Physics and Astronomy, University of North Carolina at Chapel Hill.

[§] Department of Physics, Duke University.

^{||} Present address: GE Global Research Center, Niskayuna, NY 12309.

[⊥] Present address: U.S. Army Aviation & Missile Research, Development & Engineering Center, Redstone Arsenal, AL 35898.

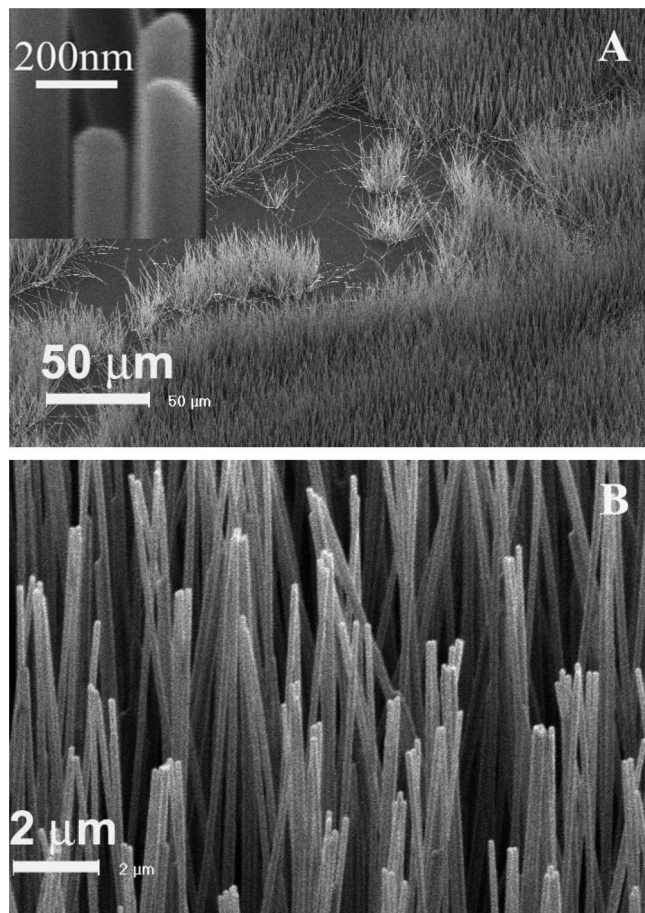


Figure 1. (A) Low-magnification FESEM image of the wafer-scale vertically aligned ZnO nanowire arrays grown on an amorphous SiO₂ substrate ~ 6 cm downstream from the precursor. Inset: High-magnification FESEM image of the nanowire tips. (B) High-magnification FESEM image of the vertically aligned ZnO nanowire arrays.

and 2 parts concentrated H₂SO₄). Then the as-grown ZnO nanowires were removed from the substrate by an ultrasonic cleaner to form a suspension in acetone, and the suspensions were dispersed on the cleaned wafers. Next, poly(methyl methacrylate) (PMMA, MW = 200000 and MW = 950000) resist layers were spin-coated on the wafers, and patterns were defined on the resist layers by electron irradiation carried out in a FESEM (Philips FEI XL30SFEG) at 30 kV. The resists were developed with a 1:3 methyl isobutyl ketone (MIBK)/isopropanol solution, then Cr/Au (15/45 nm) films were thermally evaporated on the resist, and final pattern formation was accomplished by lift-off in acetone. Electrical transport source–drain measurements were performed at room temperature on a home-built system.

Results and Discussion

Figure 1A is a representative low-magnification FESEM image of the as-grown high-density ZnO nanowire arrays grown at 882 °C on a substrate located ~ 6 cm downstream from the precursor material. High-magnification FESEM (Figure 1B) indicates that the corresponding diameters of the ZnO nanowires are nearly monodisperse at ~ 100 nm. The arrays are composed of vertically aligned nanowires up to 45 μm long, densely packed over large areas where catalysts covered the SiO₂ substrate. For this study, Ni(NO₃)₂ deposited on the substrate resolves into a NiO film (Figure 2) that serves as the catalyst for growth of the aligned ZnO nanowires.

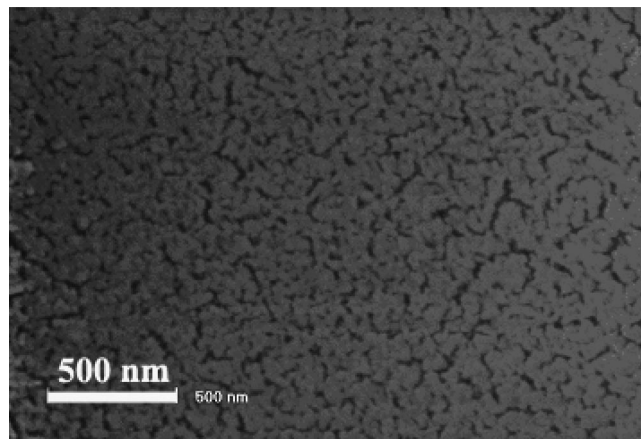


Figure 2. FESEM image of a NiO film patterned substrate, prepared by putting a Ni(NO₃)₂-patterned substrate at a distance of ~ 8 cm from center of the furnace and then annealing the substrate with a center temperature of 900 °C for 4 h under a steady, 150 sccm flow of argon.

When the distance between the substrate and the precursor material was increased, the substrate temperature could be easily controlled. We found that there was a correlation between substrate temperatures and the diameters and lengths of the vertically aligned ZnO nanowires. For example, compare the FESEM images shown in Figures 1 and 3A. Both samples were grown simultaneously in the same run, but the substrate in Figure 3A was located ~ 10 cm downstream from the precursor material with a growth temperature of 833 °C. The diameters of these nanowires range from 260 to 400 nm with an average diameter (~ 340 nm) more than three times that of the nanowires in Figure 1. Conversely, the nanowires grown at higher temperature (Figure 1) are up to 45 μm long, while those grown at lower temperature (Figure 3A) are only ~ 4 μm long. There is a remarkably linear relationship between growth distance (i.e., temperature) and nanowire diameter (Figure 3B); however, the polydispersity of the nanowire diameters increased with decreasing growth temperature.

X-ray diffraction (XRD) investigations of the overall crystallographic properties and phase purity reveal that the nanowires have a pure hexagonal (wurtzitic) ZnO phase. A typical measured XRD pattern (Figure 4A) can be indexed to a wurtzitic ZnO crystalline structure that matches well with the standard lattice constants of $a = 0.3250$ nm and $c = 0.5207$ nm (Joint Committee on Powder Diffraction Standards (JCPDS) Card No. 36-1451). The presence of a strong (002) diffraction peak and the absence of other peaks (e.g., (110) peak is too weak to be seen) confirm that the vertically aligned ZnO nanowires are preferentially oriented along the [001] direction. A structural model of the vertically aligned ZnO nanowires is illustrated in Figure 4B. These observations are confirmed by measured high-resolution TEM (HRTEM) images and selected area electron diffraction (SAED) patterns. Figure 5A is an HRTEM image recorded from a ZnO nanowire that clearly reveals the (001) atomic planes with an interplanar spacing of 0.52 nm along the length of the nanowire. The SAED pattern (inset of Figure 5A) recorded along the [100] zone axis confirms the wurtzitic structure with the same lattice constants obtained from XRD.

Growth of one-dimensional nanowires usually proceeds by one of two processes: the vapor–liquid–solid (VLS)²⁸ or the vapor–solid (VS)²⁹ mechanism. In the VLS mechanism, a catalyst is required, and remnant catalyst particles are typically attached to tips of the one-dimensional nanostructures.²⁸ By

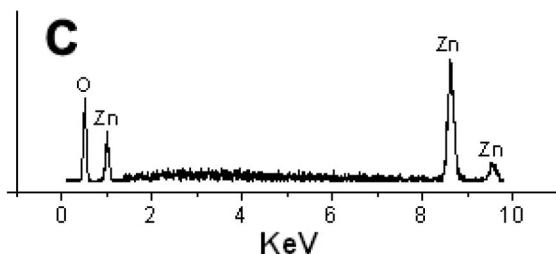
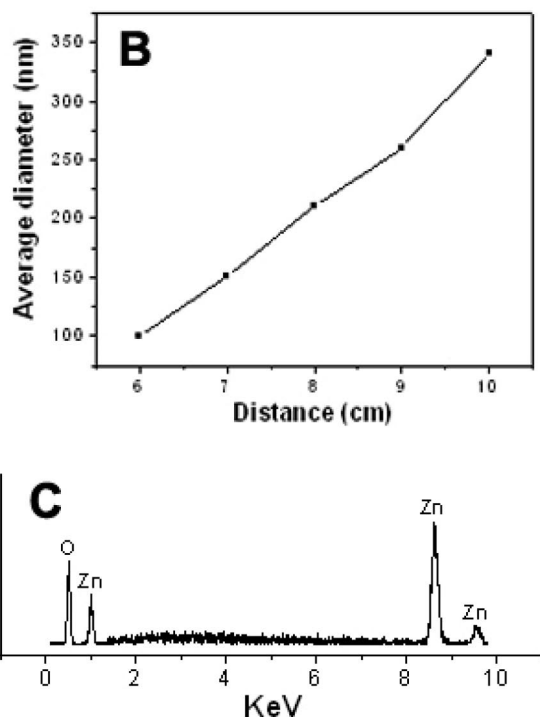
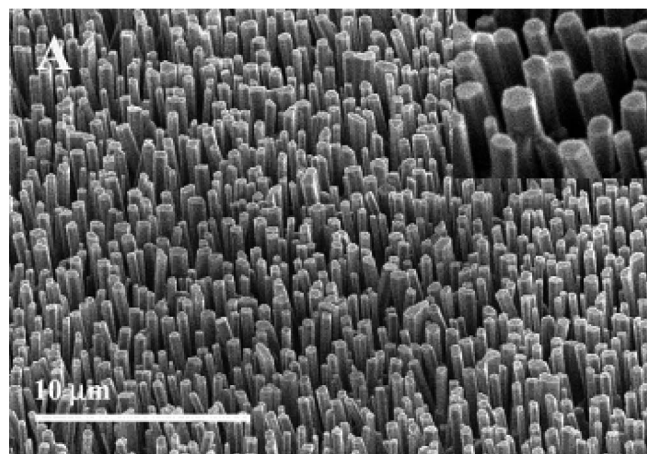


Figure 3. (A) FESEM image of vertically aligned ZnO nanowire arrays, grown simultaneously with the samples shown in Figure 1 but ~ 10 cm downstream from the precursor. Inset: Magnified FESEM image of the nanowires' hexagonal tips, clearly showing the absence of catalyst particles. (B) Linear relationship between the nanowire's average diameter and the precursor-substrate distance. (C) Energy dispersive X-ray spectrum of the ZnO nanowire tips, showing no detected catalyst elements, only Zn and O with a ratio of 1:1.

contrast, the VS mechanism does not require a catalyst. To ascertain which mechanism operated during the growth of the vertically oriented ZnO nanowires reported here, HRTEM images of the nanowire tips were obtained. Although the nanowires grew only at locations with catalysts (Figure 1A), neither catalyst particles nor catalyst components were detected at the tips of the ZnO nanowires. Note the absence of catalytic nanoparticles and bare hexagonal shape of the nanowire tips in the FESEM images of Figures 1B and 3A, as well as the clean ZnO planes in the HRTEM image of nanowire tips in Figure 5B. EDX focused on the nanowire tip region (Figure 3C) reveals no elements but Zn and O, whose ratio is the expected 1:1. Thus, catalysts are required for the growth, but there are no catalysts on the tips of the nanowires, so neither VLS nor VS adequately describes the growth.

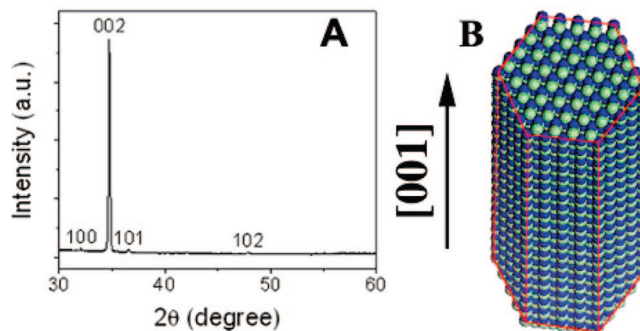


Figure 4. (A) Room temperature XRD pattern of the vertically aligned ZnO nanowire arrays measured using Cu K α radiation. (B) Structure model of the vertically aligned ZnO nanowires.

Recently, similar observations were made regarding the growth of AlN nanowires also catalyzed by Ni.³⁵ We posit the “vapor–solid epitaxial (VSE) mechanism” proposed to explain AlN nanowire growth to explain the growth of ZnO nanowires here. The VSE mechanism proceeds as follows. Ni(NO₃)₂ deposited at high temperature on the substrate becomes a NiO film that catalyzes growth of the nanowires. For ZnO nanowires, ZnO vapor produced at the center of furnace is continuously transported downstream by the flow of argon gas to a lower temperature zone where the substrates are located. Vapor-phase ZnO adsorbs on the energetically favored sites on the NiO film until the resulting ZnO film reaches a critical thickness. After that, the inherent strain induced by the lattice mismatch between the ZnO and NiO films causes the formation of ZnO nanocrystals that serve as nucleation sites for the subsequent growth. Because wurtzite structure has no center of inversion, an inherent asymmetry along the *c* axis is present which allows the preferential growth of the nanocrystal along the [001] direction to form nanowires.³⁰ As shown in Figure 1A, the nanowires on the boundaries of the arrays are less vertically oriented than the nanowires within the boundaries of the arrays. Thus, vertical alignment appears to be maintained by interactions among the densely grown ZnO nanowires and the rigidity of the ZnO nanowires.

To explain the increase in nanowire average diameter and polydispersity with increasing distance between precursors and substrates, note that the precursors are located at the hottest region of the growth chamber, the center. The farther away the substrate is from the precursor, the cooler the growth region is. Smaller diameter, monodisperse nanowires were grown on the hottest substrates while the larger diameter, polydisperse nanowires were grown on increasingly cooler substrates. This suggests that the size and polydispersity of the nucleating nanocrystals, which form at locations to relieve strain, increases with decreasing substrate temperature. At high substrate temperatures, rapid nanowire growth begins immediately after nanocrystal formation, freezing in the minimum nanocrystal/nanowire diameter. For decreasing substrate temperature, the nanocrystals have a greater opportunity to grow laterally in order to distribute strain relief before vertical nanowire growth begins. In all cases, once vertical growth begins, further lateral growth ceases, and growth temperature governs the length of the nanowire.

Figure 6 shows room temperature PL spectra of the ZnO nanowire arrays. Curves A and B are the PL spectra measured from nanowire arrays with 100 nm (i.e., Figure 1) and 340 nm (i.e., Figure 3a) average diameters, respectively. The emission at ~ 3.24 eV, near the ultraviolet (UV) band edge emission of ZnO (~ 3.3 eV at 295 K),³¹ is generally attributed to the recombination of free excitons through an exciton–exciton

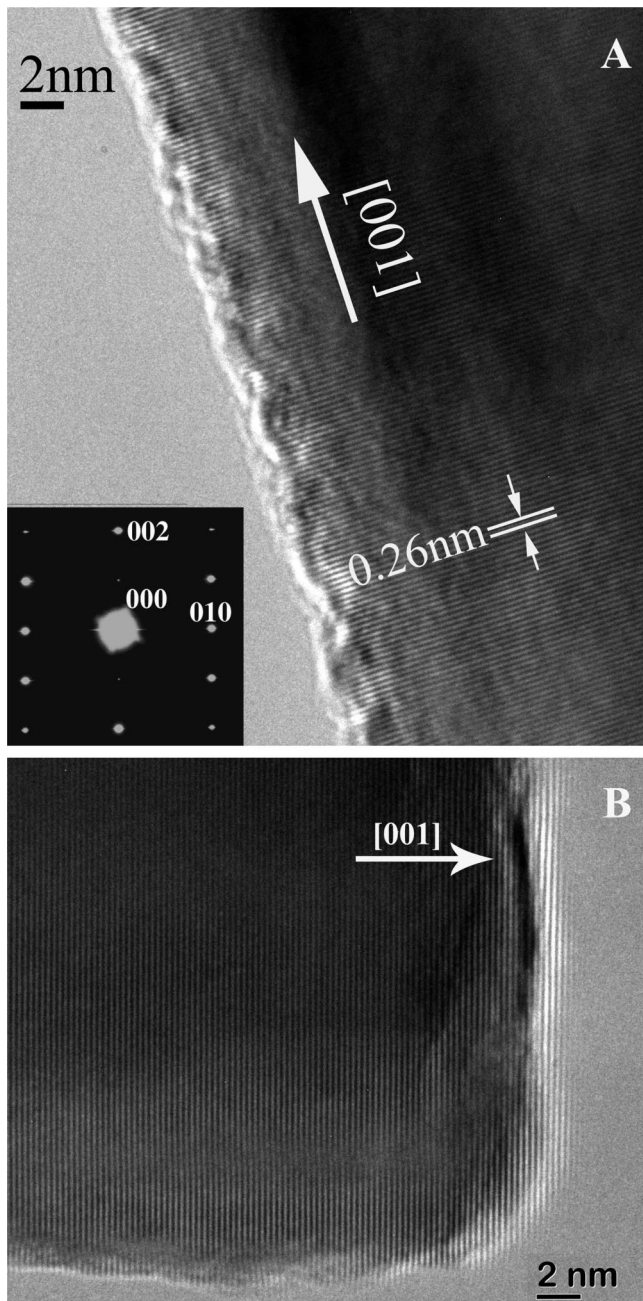


Figure 5. (A) HRTEM image recorded from a ZnO nanowire, showing the nanowire growing along [001] direction. Inset: SAED patterns of the nanowire recorded along [100] zone axis. (B) HRTEM image recorded from the ZnO nanowire tip.

collision process.¹ The broad, below band gap “green band” visible wavelength emission, centered at 2.57 eV, has been attributed to the recombination of trapped holes with free electrons in ZnO.³² The traps responsible for green band emission are believed to be concentrated near the surface, so the increased surface-to-volume ratio of nano-ZnO, as compared to bulk or thin films, increases the peak intensity ratio of the green band emission to the UV band edge emission.^{4,31,33} This dependence of green band emission on nanowire diameter is observed for the vertically aligned ZnO nanowires reported here: the intensity of the green band emission is stronger than that of the UV band edge emission for the 100 nm diameter nanowires (curve A) and vice versa for the 340 nm diameter nanowires (curve B).

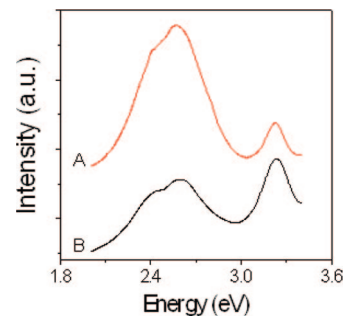


Figure 6. Room temperature photoluminescence spectra of the vertically aligned ZnO nanowire arrays with excitation energy of 3.815 eV.

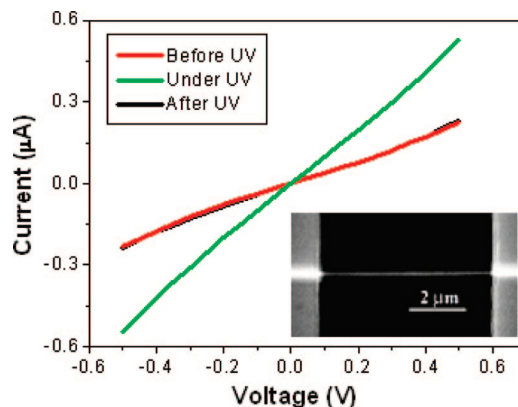


Figure 7. Room temperature I – V results of an individual ZnO nanowire device measured with and without UV illumination (the red line (Before UV) overlaps with the black line (After UV)). Inset: FESEM image of the individual ZnO nanowire device.

To measure the electrical properties of individual ZnO nanowires, test devices were fabricated by the e-beam lithographic technique described above. Figure 7 presents the room temperature I – V results of an individual ZnO nanowire device measured in air with and without UV illumination (UVG-54 mineralight Lamp, 115V, 60 Hz, 0.16 A) at a photon energy (4.88 eV, $\lambda = 254$ nm) large enough to excite electrons across the band gap of ZnO (3.37 eV). The inset of Figure 7 is a FESEM image of the ZnO single nanowire (100 nm diameter) device. The conductivity of the UV-illuminated nanowire greatly increased due to the photogenerated carriers in the semiconducting ZnO nanowire but returned to its original value when UV illumination was turned off, indicating their potential as inexpensive UV light nanosensors. Furthermore, the resistivity of the ZnO nanowires measured in air was found to increase with decreasing nanowire diameter, an effect that may have two causes. First, it may be another consequence of the increasing fractional volume of green band traps with decreasing diameter. Second, it may be due to the formation of O_2^- from surface-adsorbed O_2 that captures a conduction band electron.^{34–36} Both mechanisms decrease carrier density and increase resistance in a manner that becomes more effective as nanowires narrow because of the increasing surface-to-volume ratio.

Conclusions

In summary, a facile, template-free method was used to grow large areas (>1 cm²) of vertically aligned dense ZnO nanowire arrays on amorphous SiO₂ substrates. Adjusting growth temperature by simply changing the distance between the precursor material and the substrate easily controlled the diameters of the ZnO nanowires. The structure of the nanowires was characterized by means of X-ray diffraction, HRTEM, and SAED, and

the results indicate the arrays are composed of single-crystalline wurtzitic ZnO nanowires grown in the [001] direction. A vapor–solid epitaxial mechanism is proposed to explain the growth of the arrays and how the nanowire diameter and length vary with substrate temperature. Photoluminescence spectra and electrical conductivity measurements indicate that broad visible wavelength luminescence and resistivity both increase as the nanowire radius decreases. Photoconductivity measurements of individual ZnO nanowire devices indicate their potential for UV nanosensors. We believe our facile and inexpensive approach for large-scale growth of vertically aligned dense ZnO nanowire arrays will open up more opportunities for fundamental studies and facilitate the development of numerous nanodevice applications.

Acknowledgment. This work is supported in part by Grant #49620-02-1-0188 from AFOSR. H.O.E. acknowledges helpful discussions with John V. Foreman.

References and Notes

- Huang, M. H.; Mao, S.; Feick, H.; Yan, H. Q.; Wu, Y.; Kind, H.; Weber, E.; Russo, R.; Yang, P. D. *Science* **2001**, *292*, 1897.
- Wong, E. M.; Searson, P. C. *Appl. Phys. Lett.* **1999**, *74*, 2939.
- Choopun, S.; Vispute, R. D.; Noch, W.; Balsamo, A.; Sharma, R. P.; Venkatesan, T.; Iliadis, A.; Look, D. C. *Appl. Phys. Lett.* **1999**, *75*, 3947.
- Huang, M. H.; Wu, Y. Y.; Feick, H.; Tran, N.; Weber, E.; Yang, P. D. *Adv. Mater.* **2001**, *13*, 113.
- Lao, J. Y.; Wen, J. G.; Zen, Z. F. *Nano Lett.* **2002**, *2*, 1287.
- Liu, B.; Zeng, H. C. *J. Am. Chem. Soc.* **2003**, *125*, 4430.
- Yin, M.; Gu, Y.; Kuskovsky, I. L.; Andelman, T.; Zhu, Y. M.; Neumark, G. F.; O'Brien, S. *J. Am. Chem. Soc.* **2004**, *126*, 6206.
- Wang, X. D.; Summers, C. J.; Wang, Z. L. *Nano Lett.* **2004**, *4*, 423.
- Geng, C.; Jiang, Y.; Yao, Y.; Meng, X.; Zapien, J. A.; Lee, C. S.; Lifshitz, Y.; Lee, S. T. *Adv. Funct. Mater.* **2004**, *14*, 589.
- Lao, J. Y.; Huang, J. Y.; Wang, D. Z.; Zen, Z. F. *Nano Lett.* **2003**, *3*, 235.
- Johnson, J. C.; Knutsen, K. P.; Yan, H. Q.; Law, M.; Zhang, Y. F.; Yang, P. D.; Saykally, R. *Nano Lett.* **2004**, *4*, 197.
- Kong, X. Y.; Ding, Y.; Yang, R. S.; Wand, Z. L. *Science* **2004**, *303*, 1348.
- Gao, P. X.; Ding, Y.; Mai, W. J.; Hughes, W. L.; Lao, C. S.; Wang, Z. L. *Science* **2005**, *309*, 1700.
- Wang, Z. L.; Kong, X. Y.; Ding, Y.; Gao, P. X.; Huges, W. L.; Yang, R. S.; Zhang, Y. *Adv. Funct. Mater.* **2004**, *14*, 944.
- Law, M.; Greene, L. E.; Johnson, J. C.; Saykally, R.; Yang, P. D. *Nat. Mater.* **2005**, *4*, 455.
- Wand, Z. L.; Song, J. H. *Science* **2006**, *312*, 242.
- Lyu, S. C.; Zhang, Y.; Lee, C. J.; Ruh, H.; Lee, H. J. *Chem. Mater.* **2003**, *15*, 3294.
- Greece, L. E.; Law, M.; Goldberger, J.; Kim, F.; Johnson, J. C.; Zhang, Y. F.; Saykally, R. J.; Yang, P. D. *Angew. Chem., Int. Ed.* **2003**, *42*, 3031.
- Chik, H.; Cloutier, S. G.; Kouklin, N.; Xu, J. M. *Appl. Phys. Lett.* **2004**, *84*, 3376.
- Park, W. I.; Yi, G. *Adv. Mater.* **2004**, *16*, 87.
- Wu, J.; Wen, H.; Tseng, C.; Liu, S. *Adv. Funct. Mater.* **2004**, *14*, 806.
- Greece, L. E.; Law, M.; Tan, D. H.; Montano, M.; Goldberger, J.; Somorjai, G.; Yang, P. D. *Nano Lett.* **2005**, *5*, 1231.
- Cui, J. B.; Gibson, U. J. *Appl. Phys. Lett.* **2005**, *87*, 133108.
- He, J. H.; Hsu, J. H.; Wang, C. W.; Lin, H. N.; Chen, L. J.; Wang, Z. L. *J. Phys. Chem. B* **2006**, *110*, 50.
- Xiang, B.; Wang, P. W.; Zhang, X. Z.; Dayeh, S. A.; Aplin, D. P. P.; Soci, C.; Yu, D. P.; Wang, D. L. *Nano Lett.* **2007**, *7*, 323.
- Li, J. Y.; Lu, C. G.; Maynor, W.; Huang, S. M.; Liu, J. *Chem. Mater.* **2004**, *16*, 1633.
- Li, J. Y.; An, L.; Lu, C. G.; Liu, J. *Nano Lett.* **2006**, *6*, 148.
- Morales, A. M.; Lieber, C. M. *Science* **1998**, *279*, 208.
- Liu, C.; Hu, Z.; Wu, Q.; Wang, X. Z.; Chen, Y.; Sang, H.; Zhu, J. M.; Deng, S. Z.; Xu, N. S. *J. Am. Chem. Soc.* **2005**, *127*, 1318.
- Wu, Q.; Hu, Z.; Wang, X. Z.; Lu, Y. N.; Chen, X.; Xu, H.; Chen, Y. *J. Am. Chem. Soc.* **2003**, *125*, 10176.
- Foreman, J. V.; Li, J. Y.; Peng, H. Y.; Choi, S. J.; Everitt, H. O.; Liu, J. *Nano Lett.* **2006**, *6*, 1126.
- Foreman, J. V.; Everitt, H. O.; Yang, J. Q.; Liu, J. *SPIE OPTO* **2009**7214–4.
- Shalish, I.; Temkin, H.; Narayanamurti, V. *Phys. Rev. B* **2004**, *69*, 245401.
- Wan, Q.; Li, Q. H.; Chen, Y. J.; Wang, T. H.; He, X. L.; Li, P. J.; Lin, C. L. *Appl. Phys. Lett.* **2004**, *84*, 3654.
- Li, Q. H.; Liang, Y. X.; Wan, Q.; Wang, T. H. *Appl. Phys. Lett.* **2004**, *85*, 6389.
- Fan, Z. Y.; Wang, D. W.; Chang, P. C.; Tseng, W. Y.; Lu, J. G. *Appl. Phys. Lett.* **2004**, *85*, 5923.

JP8083716